Conformational Features of Group-4 *ansa*-Metallocenes with Long $-(CH_2)_n-$ Chains Connecting Their Cyclopentadienyl Ligands

Tim Jödicke,[a][‡] Frederik Menges,[a] Gerald Kehr,[a] Gerhard Erker,*[a] Udo Höweler,[a][‡] and Roland Fröhlich[a][‡‡]

Keywords: Metallocenes / Zirconium / Conformation analysis / Density functional calculations / Polymerization

Treatment of 1,9-bis(lithiocyclopentadienyl)nonane (**8b**) with $ZrCl_4(THF)_2$, in dilute solution, gave the crystalline mononuclear "large" *ansa*-metallocene **3b** (7% isolated). The X-ray crystal structure analysis of **3b** revealed a metallocene conformation where the nonamethylene bridge is oriented toward the lateral sector of the bent metallocene wedge. An analogous structure of **3b** is probable in solution, as shown by dynamic ^1H NMR spectroscopy. The activation barrier for the metallocene conformational equilibration process of **3b** was determined as $\Delta G^{\ddagger}_{rot}$ (203 K) = 8.8 ± 0.3 kcal/mol in [D_8]toluene. A combination of force-field and DFT calculations revealed similar conformational minima for **3b** and a series of related "large" *ansa*-metallocene complexes in the gas phase. The corresponding complex $[(CH_2)_{12}(C_5H_4)_2]ZrCl_2$ (**3d**) was also prepared. When activated by treatment with methylalumoxane, both complexes **3b** and **3d** give very active metallocene Ziegler–Natta catalysts for the polymerization of ethene and the oligomerization of propene.

Introduction

A specific section of the many possible group-4 *ansa*-metallocenes has become of great importance in homogeneous catalysis. These systems usually exhibit small bridges (i.e. R_2Si, R_2C or $-CH_2-CH_2-$) between a pair of Cp, indenyl, or related ligands. They have formed the basis for the generation of homogenous Ziegler−Natta-type catalysts, which often show extraordinary reactivity/selectivity features.[1] Such systems are conformationally rigid with the "*ansa* bridge" strictly located at the narrow back side of the bent metallocene wedge. This seems to be a key factor for their controlling abilities in the actual catalytic process.[2,3] Open, non-bridged group-4 metallocenes have also been shown to lead to active Ziegler−Natta catalysts. Here, control of the stereoselectivity of polyolefin formation is sometimes achieved, based on the specific dynamic conformational properties of the alkyl- or aryl-substituted bent metallocene system.[4,5]

"Large" *ansa*-metallocenes, which have their cyclopentadienyl or indenyl ligands connected by long $-(CH_2)_n-$ chains ($n \geq$ ca. 8), comprise an interesting class of compounds. It is possible that some members of this group form stable global (or kinetically protected local) conformational minima that have the oligomethylene chain located at specific sectors of the bent metallocene wedge, where they may actively shield the active sites at the central metal center, or may get involved in reactions taking place at the activated group-4 metal inside this arrangement.[6] A long bridging $-(CH_2)_n-$ chain in a "large" *ansa*-metallocene could, for instance, be located symmetrically at the front of the bent metallocene wedge and spatially separate the space in front of the activated metal center. This may potentially alter the catalytic action in such a system relative to a less-restricted non-bridged metallocene or a conventional "small" *ansa*-metallocene system.

To the best of our knowledge, only two examples of such "large" *ansa*-metallocenes have been characterized by X-ray diffraction so far, and these show very different conformational features. Mach et al. have described the structure of $[(CH_2)_8Cp^*_2]TiCl_2$ (**1**, see Figure 1) which has the bridging octamethylene chain located at the narrow back side, almost like a "small" *ansa*-metallocene.[7] In contrast, in *rac*-$[(CH_2)_{12}(1\text{-indenyl})_2]ZrCl_2$ (*rac*-**2c**), the other previously described example, the bridging hydrocarbyl chain is C_2-symmetrically located at the front of the bent metallocene wedge.[8] This bisects the Cl−Zr−Cl angle as shown in the bottom projection in Figure 1.

From the static solid-state structures it is not clear whether these two forms represent the respective global conformers of these bent metallocenes, or if they are just local conformational minima that have been stabilized by specific solid-state features under these experimental conditions. Thus, we have characterized several representative "large" *ansa*-metallocenes, i.e. $(CH_2)_n$-bridged bis(cyclopentadienyl) or bis(indenyl) complexes of zirconium (and in one case titanium) with the number of bridging methylene units ranging from eight to twelve, by computational chemistry using force-field and DFT methods. We have found a remarkable dependence of the thermodynamically favored metallocene conformations on the length of the oligomethylene bridge. These results were complemented experimentally by the synthesis of two representative "large" *ansa*-zirconocene dichlorides, the investigation of their respective

[a] Organisch-Chemisches Institut der Universität Münster, Corrensstraße 40, 48149 Münster, Germany
[‡] Theoretical work.
[‡‡] X-ray crystal structure analysis.
Supporting information for this article is available on the WWW under http://www.wiley-vch.de/home/eurjic or from the author.

  1434−1948/01/0808−2097 $ 17.50+.50/0

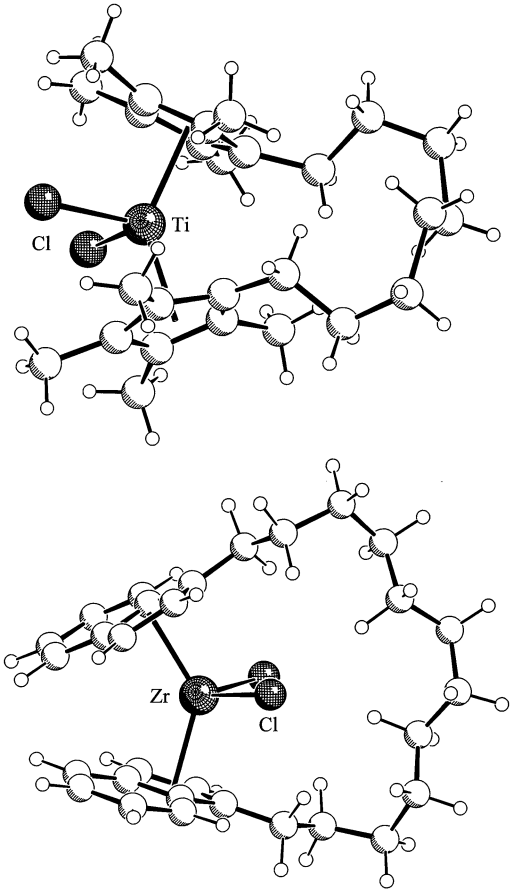

Figure 1. SCHAKAL plots of the "large" *ansa*-metallocenes **1** (top) and *rac*-**2c** (bottom), that were previously described in the literature[7,8]

dynamic conformational interconversion in solution, and the structural characterization of one example by X-ray diffraction. This has provided us with a much more detailed picture of the conformational properties of the interesting group-4 "large" *ansa*-metallocene complexes, relative to the selected views derived from previous descriptions based only on a limited number of experimental observations.

Results and Discussion

Computational Studies

The various local conformational minima of a series of $[(CH_2)_n(C_5H_4)_2]ZrCl_2$ complexes **3a**−**d** (n = 8, 9, 10, and 12) were determined and optimized using a metallocene-adapted force-field method that we had described and applied previously (see Scheme 1).[9] Relative energies of the located conformers were determined. These geometries were then used in the DFT calculation to give the respective single-point energies on the B3LYP level[10] for comparative purposes. We made sure that the conformational characteristics were predominately determined by the bent metallocene framework itself and not by the σ-substituents attached at the zirconium atom. This was done by investigating several corresponding $[(CH_2)_n(C_5H_4)_2]Zr(CH_3)_2$ complexes **4a**−**d** with the same number of bridging methylene groups. The Zr−C(sp^3) parameterization of the organometallic molecular modeling/force-field program was carried out in the course of this study (see Exp. Sect.). In addition, a similar series of *rac*- and *meso*-$[(CH_2)_n(1\text{-indenyl})_2]ZrCl_2$ complexes (*rac*-/*meso*-**2a**−**c**, n = 8, 10, and 12) was investigated by this combination of force-field/DFT calculations, and the Ti-based system **1** recently described by K. Mach et al. (see above),[7] was included in the study for comparison.

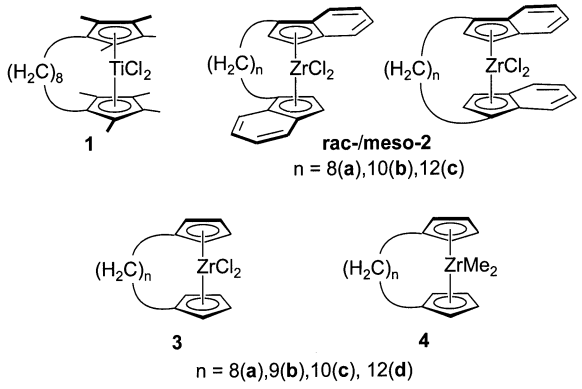

Scheme 1. "Large" *ansa*-metallocene complexes calculated by force-field and DFT methods in this study

For clarity and simplicity we want to characterize the metallocene conformations using a grid (see Figure 2) that is superimposed on a projection of the bent metallocene from the top. In this projection, the bent metallocene opens towards the right, with its σ-substituents directed toward the "east" position. In the center of that position we will place the origin of the conformational designation (i.e. 0°), we will then proceed clockwise through the "south" (90°), "west" (180°), and "north" (−90°) positions back to the origin. In the designation of a specific metallocene conformation (denoted by *mc*), we will first note the position of the Cp−CH_2− vector of the upper substituted cyclopentadienyl (or indenyl) ligand, followed by that of the lower C(Cp)−CH_2− position in degrees in this reticule, which has its center (idealized) position superimposed with the Cp(centroid)−Cp(centroid) vector. The structurally characterized examples **1** and *rac*-**2c** (see Figure 1) are thus characterized by the metallocene conformational descriptors *mc* 159/−159 (M = Ti, n = 8) and *mc* 16/−18 (M = Zr, n = 12).

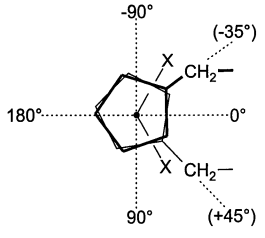

Figure 2. Reticule used for the characterization of the bent metallocene conformers; the specific example depicted would be termed as the *mc* −35/45 conformation

The molecular mechanics calculation has revealed that *rac*-**2c** is characterized by a very shallow conformational hypersurface. A variety of metallocene conformations with very similar energies were found that represent local minima on the conformational surface. The local minima of *rac*-**2c** with the lowest energies, exhibiting the oligomethylene chain predominantly in the "front", "lateral" or "back" sector of the bent metallocene wedge are listed in Table 1. The force-field calculations locate the global minimum conformation (*mc* 9/−9) with an orientation that is very close to the experimental X-ray structure of *rac*-**2c** (see Figure 1), with a structurally even closer conformation (*mc* 16/−16) close by. However, it must be noted that several other structurally different conformational minima of *rac*-**2c**, with only slightly higher energies, were found in this calculation (see Table 1). The overall picture is supported by the result of the DFT calculation. An optimized global minimum structure (*mc* 19/−19) is calculated (see Table 1), that is structurally marginally different from the observed experimental structure of *rac*-**2c**.

The situation changes systematically when the oligomethylene chain is shortened. The decamethylene-bridged system *rac*-**2b** exhibits a set of preferred "lateral" conformations as the global minimum (e.g. *mc* 74/137), whereas the orientation of the $-(CH_2)_{10}-$ bridge at the "front" side is markedly disfavored for the hypothetical system *rac*-**2b** according to this force-field calculation. This situation becomes consistently more pronounced on further shortening of the oligomethylene chain. In *rac*-**2a**, the $-(CH_2)_8-$ chain is preferentially located laterally (global minimum *mc* 85/

Table 1. Calculated metallocene conformations of the *rac*- and *meso*-[$(CH_2)_n$(1-indenyl)$_2$]$ZrCl_2$ complexes **2**

Compound	*n*	Conformation type	Relative energy MM[a]	Relative energy (*mc*)	Relative energy DFT[b]	Relative energy (*mc*)
rac-**2a**	8	"lateral"	0.0	(97/128)	0.0	(85/123)
			1.4	(82/113)	0.8	(85/128)
			1.9	(78/81)	3.3	(85/89)
		"back"	5.0	(140/−143)		[c]
		"front"	22.6	(4/−19)	17.5	(4/−21)
rac-**2b**	10	"lateral"	0.0	(74/137)	0.0	[d]
			0.1	(77/115)	−0.2	[d]
			0.2	(50/75)	0.7	[d]
		"back"	2.4	(109/−146)	5.2	[d]
			3.7	(142/−142)	4.3	[d]
		"front"	7.5	(10/21)	11.0	[d]
			4.7	(1/−11)	7.7	[d]
rac-**2c**	12	"lateral"	0.0	(85/111)	0.0	(83/116)
			0.0	(42/130)	1.1	(79/119)
			0.1	(39/123)	0.9	(57/89)
			0.1	(40/133)	0.1	(58/80)
		"back"	0.4	(105/−129)	3.2	(97/−134)
		"front"	−1.1	(9/−9)	−2.3	(19/−19)
			−0.3	(16/−16)	−1.8	(24/−24)
		"gauche"	−0.2	(2/93)	0.8	(5/88)
rac-**2c**	12	experiment:[e]		(16/−18)	–	–
meso-**2a**	8	"lateral"	0.0	(97/128)	0.0	(89/129)
			0.7	(65/91)	3.4	(73/96)
			1.9	(78/81)	3.3	(85/89)
		"back"	13.7	(140/−143)	14.4	(124/−151)
		"front"	17.0	(0/−27)	18.9	(10/−17)
			22.8	(6/29)	19.2	(3/7)
meso-**2b**	10	"lateral"	0.0	(72/105)	0.0	[d]
			0.2	(46/81)	2.4	[d]
			0.3	(50/75)	0.0	[d]
		"back"	7.2	(132/176)	9.4	[d]
			7.6	(141/−151)	8.8	[d]
			6.2	(134/−145)	6.3	[d]
		"front"	7.9	(17/−23)	8.5	[d]
			6.2	(10/−29)	7.4	[d]
meso-**2c**	12	"lateral"	0.0	(36/78)	0.0	(50/85)
			0.3	(83/139)	1.0	(80/122)
			0.4	(42/130)	1.9	(49/136)
		"back"	0.8	(111/−110)	1.5	(95/−133)
		"front"	2.0	(9/−32)	1.0	(22/−24)
			1.4	(12/−27)	0.0	(22/−25)
		"gauche"	0.1	(−2/93)	−0.6	(−6/88)

[a] Energy relative to the most stable "lateral" conformation, metallocene force field [kcal mol^{-1}]. – [b] B3LYP-optimized [kcal mol^{-1}]. – [c] No minimum found. – [d] B3LYP single point energies [kcal mol^{-1}] of the calculated force-field structure. – [e] From ref.[8]

123 by the B3LYP-DFT calculation, *mc* 97/128 by our metallocene force-field method), and the "front" orientation is strongly disfavored (see Table 1). A similar picture is found in the force-field and DFT calculations of the corresponding *meso*-[−$(CH_2)_n$−(1-indenyl)$_2$]$ZrCl_2$ systems, *meso*-**2a**−**c** (n = 8, 10, 12, see Table 1).

These results showed that the DFT calculations are very good at predicting the preferred conformations of "large" *ansa*-metallocenes. Furthermore, the much simpler metallocene force-field investigation gave quite acceptable results. Therefore, we used both methods for a priori characterization of the preferred metallocene conformations of the parent [$(CH_2)_n(\eta^5$-$C_5H_4)_2$]$ZrCl_2$ "large" *ansa*-zirconocene dichloride complexes **3a**−**d** (n = 8, 9, 10, and 12). A similar trend as in the *rac*-/*meso*-**2** series of complexes is observed here. The smaller members of the series [**3a** (n = 8), **3b** (n = 9), **3c** (n = 10)] all favor metallocene conformations that exhibit a "lateral" orientation of the oligomethylene bridge. However, the difference in energy between the preferred "lateral" conformation and the less favored "back" and "front" arrangements decreases progressively from **3a** to **3c**. Eventually, the cross-over point is reached with complex **3d** (n = 12), where the energy difference between the "front" and "lateral" arrangements becomes marginal (actually, the "front" orientation of the −$(CH_2)_{12}$− chain is slightly favored by the DFT calculation, see Table 2).

The complex **3b** (n = 9) has been synthesized and its molecular structure in the crystal has been determined (see below). The experimentally observed "lateral" orientation of the bridging nonamethylene chain is characterized by the metallocene conformational descriptor *mc* 83/83 (see Figure 2). The force-field-calculated global-minimum structure has an *mc* of 78/81, the DFT (B3LYP) global minimum has an *mc* of 77/83. This is a remarkably accurate structural coincidence in such a flexible conformational system. This result highlights the high predictive potential of both computational chemistry methods used in this investigation.[11]

We have also characterized the preferred metallocene conformations of the members of the corresponding series of [$(CH_2)_n(\eta^5$-$C_5H_4)_2$]$Zr(CH_3)_2$ complexes **4a**−**d** (n = 8, 9, 10, and 12), using our newly parameterized metallocene force-field program. The structural preferences were very similar to the [$(CH_2)_n(\eta^5$-$C_5H_4)_2$]$ZrCl_2$ series (see above). We therefore refer to the Supporting Information for the details of this study.

Finally, we have analyzed the titanium system **1**. It can be seen from Table 3 that in this case the force-field method does not reproduce the observed metallocene conformation.

Table 2. Calculated metallocene conformations of the [$(CH_2)_n(\eta^5$-$C_5H_4)_2$]$ZrCl_2$ complexes **3**

Compound	n	Configuration type	Relative energy MM[a]	(*mc*)	Relative energy DFT[b]	(*mc*)
3a	8	"lateral"	0.0	(64/90)	0.3	(70/96)
			0.1	(89/115)	0.0	(84/115)
			0.9	(77/81)	0.1	(82/89)
		"back"	6.2	(137/−144)		[c]
			6.6	(149/−149)	7.3	(147/−147)
		"front"	18.4	(0/−25)	16.0	(6/−19)
3b	9	experiment:[d]		(83/83)	–	–
3b	9	"lateral"	0.0	(78/81)	0.0	(77/83)
			0.1	(69/108)	1.3	(72/113)
			0.1	(78/102)	1.7	(72/93)
			0.9	(76/104)	2.3	(81/106)
		"back"	5.2	(97/−177)	5.1	(66/127)
			5.2	(139/−143)	6.0	(125/−155)
		"front"	12.0	(2/−30)	11.9	(7/−26)
			14.1	(28/28)	12.2	(19/19)
			9.7	(2/2)	10.5	(7/7)
3c	10	"lateral"	0.0	(68/105)	0.0	(70/104)
			0.0	(45/106)	1.8	(62/115)
			0.1	(77/104)	1.4	(79/101)
			0.2	(76/104)	0.6	(81/106)
		"back"	2.3	(109/−145)	2.3	(63/151)
			2.6	(113/−145)	1.7	(60/139)
			3.7	(109/−144)	2.5	(76/142)
		"front"	6.7	(1/9)	6.2	(3/15)
3d	12	"lateral"	0.0	(82/111)	1.8	(88/121)
			0.0	(75/99)	0.0	(73/98)
			0.2	(77/84)	0.0	(76/92)
		"back"	0.1	(111/−115)	0.7	(92/−142)
		"front"	0.2	(21/−21)	−3.2	(24/−23)
			0.4	(9/−9)	−3.3	(16/−17)
		"gauche"	0.2	(3/82)	−2.6	(27/85)

[a] See footnote in Table 1. − [b] See footnote in Table 1. − [c] See footnote in Table 1. − [d] This work, see below.

Furthermore, the DFT calculation is not decisive, it reveals that the highly methyl-substituted "large" *ansa*-titanocene complex **1** is probably characterized by a very shallow conformational hypersurface. It is likely that the observed structure of **1** does not represent the global conformational minimum of the system, but rather one of the many metallocene conformations that are similar in energy, which has been stabilized by crystal packing forces in the solid state.

Table 3. Calculated and observed metallocene conformations of the "large" *ansa*-titanocene complex $[(CH_2)_8(\eta^5\text{-}C_5Me_4)_2]TiCl_2$ (**1**)

Configuration type	Relative energy MM[a]	(*mc*)	Relative energy DFT[b]	(*mc*)
"lateral"	0.0	(89/114)	0.0	(98/126)
	1.4	(63/86)	2.9	(72/95)
"back"	0.7	(126/151)	−0.5	(139/177)
	5.8	(141/−173)	1.4	(157/−158)
	16.3	(156/−153)	[c]	
"front"	15.5	(2/−34)	13.0	(2/−20)
experiment:	[d]	(159/−159)	–	–

[a] See footnote in Table 1. − [b] See footnote in Table 1. − [c] See footnote in Table 1. − [d] From ref.[7]

Experimental Studies

Previously, we and others had tried to prepare "large" *ansa*-metallocenes by coupling reactions, by means of intramolecular metallacyclopentane formation[12] using pendant alkenyl groups attached at the Cp ligands.[6,7] The metallacyclopentane formation is not problematic, but the necessary subsequent cleavage by e.g. HCl, appears to lead to the expected "large" *ansa*-metallocene product only in a limited number of cases. Mach's peralkylated *ansa*-titanocene complex **1** was actually synthesized in that way.[7] Even in the titanium systems, competing pathways leading to ring-opened acyclic products were observed. This completely dominated the protolytic cleavage in the case of the corresponding zirconocene examples, as we had recently shown.[6]

Therefore, we have chosen to synthesize the "large" *ansa*-metallocene examples used in this study using a different pathway. Starting materials were 1,9-dihydroxynonane (**5b**) or 1,12-dihydroxydodecane (**5d**), respectively. These compounds were converted into their respective dimesylates **6b** and **6d** by treatment with methanesulfonyl chloride in pyridine. Subsequent treatment with an excess of lithium cyclopentadienide resulted in clean, twofold substitution reactions, with carbon−carbon bond formation in each case, yielding 1,9- and 1,12-bis(cyclopentadienyl)nonane (**7b**, ca. 60% isolated) and -dodecane (**7d**, 86%), respectively (see Scheme 2). These two products were then deprotonated twice by treatment with *n*-butyllithium in ether. The corresponding α,ω-bis(lithiocyclopentadienyl)alkanes **8b** and **8d** were obtained almost quantitatively, as extremely insoluble solids. These dianion equivalents were only characterized by elemental analysis and by hydrolysis and deuteriolysis experiments, and then directly employed as reagents for the metathetical reaction with zirconium tetrachloride.

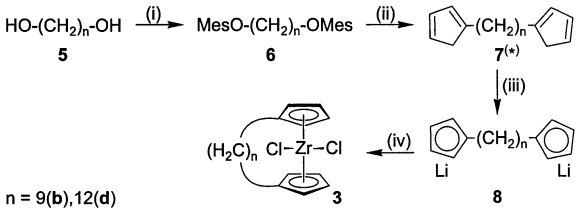

(i) CH_3SO_2Cl/pyridine; (ii) CpLi/THF; (iii) n-BuLi/Et_2O; (iv) $ZrCl_4(thf)_2$/toluene
(*) mixture of double bond isomers

Scheme 2. Syntheses of the *ansa*-metallocene complexes **3**

The reaction involving the poorly soluble $[Cp-(CH_2)_9-Cp]^{2-}(Li^+)_2$ (**8b**) was carried out with $ZrCl_4(THF)_2$ suspended in toluene. Under these circumstances, similar conditions to those used in typical high-dilution techniques[13] were obtained. The resulting product mixture nevertheless apparently contained oligomeric metallocene materials, which were highly insoluble, as the major components. Soxhlet extraction with pentane over 60 h eventually gave a soluble fraction of 1,1′-nonamethylenebis(cyclopentadienyl)zirconium dichloride (**3b**), which was obtained pure after subsequent recrystallization from toluene at −30 °C, in a 7% yield. 1,1′-Dodecamethylenebis-(cyclopentadienyl)zirconium dichloride (**3d**) was prepared analogously by treatment of the reagent **8d** with $ZrCl_4(THF)_2$, and isolated with a yield of 18%.

Crystals of complex **3b**, that were suitable for X-ray crystal structure analysis, were obtained from a benzene solution over a period of several weeks. In the solid state the nonamethylene-bridged system **3b** exhibits an eclipsed metallocene conformation that has the large *ansa* bridge oriented almost perfectly toward one lateral sector. The specific metallocene conformation can be described by the experimental metallocene conformational descriptor *mc* 83/83 (see Figure 2 and Figure 3). The chlorine atom Cl1 is disordered over two positions, therefore bonding parameters involving this atom will not be discussed in detail. The Cp(centroid)−Zr−Cp(centroid) angle in **3b** is equal to 130.6° and the averaged Cp(centroid)−Zr distance is 2.194 Å; both values are in a very typical zirconocene range {for comparison: Cp_2ZrCl_2 (129.3°/2.203 Å),[14] $[(CH_2)_3(C_5H_4)_2]ZrCl_2$ (129.5°/2.193 Å),[15] Cp_2TiCl_2 (131.0°/2.059 Å)}.[16] Only large substituents at the Cp rings result in noticeable distortions toward larger "bite angles" (and consequently smaller Cp(centroid)−Zr−Cp(centroid) angles $[(Me_3SiC_5H_4)_2ZrCl_2$ (125.4°/2.197 Å),[17] $(Me_3CC_5H_4)_2ZrCl_2$ (116.6°/2.192 Å)].[18] The opposite effect is observed for the pair of "large" *ansa*-metallocenes *rac*-**2c** [Cp(centroid)−Zr−Cp(centroid) angle 133.8°, Cp(centroid)−Zr distance 2.242 Å[8]] and **1** (137.9°/2.140 Å,[7] see Figure 1).

Thus, it appears that the $[(CH_2)_9(C_5H_4)_2]ZrCl_2$ system **3b** represents an unstrained system within the family of the "large" *ansa*-metallocenes, that can attain a normal bent metallocene core with almost no structural distortion, sim-

ilar to ordinary non-bridged $(RCp)_2MX_2$-type group-4 bent metallocene complexes. The $-(CH_2)_9-$ chain in **3b** adopts a crown-shaped cycloalkane conformation, similar to that found in many medium- and large-ring cycloalkanes (Figure 3).[19] The experimentally observed conformer of **3b** obtained in the solid state by X-ray diffraction (*mc* 83/83) is not completely identical but very similar to the probable global-minimum gas-phase structure as calculated by the force-field method (*mc* 78/81) and the DFT calculation (*mc* 77/83, see Table 2).

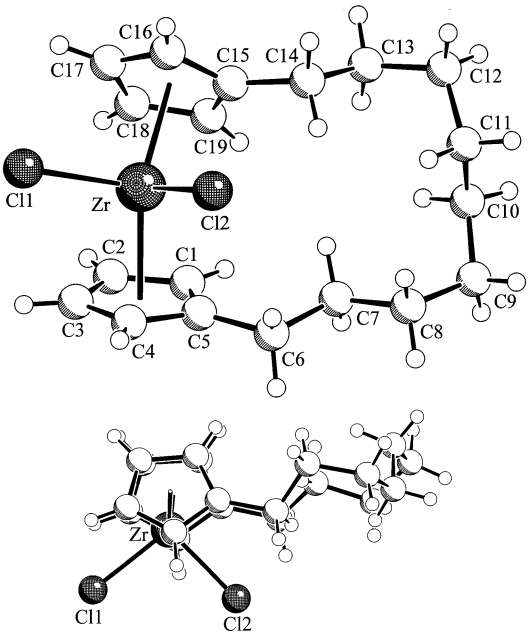

Figure 3. Two views of the molecular structure of the "large" *ansa*-metallocene **3b** in the crystal; selected bond lengths [Å], angles [°] and dihedral angles [°]: Zr−Cl1 2.424(1), Zr−Cl2 2.431(1), C1−C2 1.412(6), C1−C5 1.399(7), C2−C3 1.385(8), C3−C4 1.394(8), C4−C5 1.408(8), C5−C6 1.503(7), C6−C7 1.508(7), C7−C8 1.518(6), C8−C9 1.523(7), C9−C10 1.525(6), C10−C11 1.495(7), C11−C12 1.516(6), C12−C13 1.533(7), C13−C14 1.501(8), C14−C15 1.506(7), C15−C16 1.400(7), C15−C19 1.396(7), C16−C17 1.389(8), C17−C18 1.382(8), C18−C19 1.412(7); Cl1−Zr−Cl2 95.60(5), C5−C6−C7 113.4(4), C6−C7−C8 113.9(4), C7−C8−C9 113.2(4), C8−C9−C10 114.7(4), C9−C10−C11 114.7(4), C10−C11−C12 114.1(5), C11−C12−C13 113.9(4), C12−C13−C14 113.3(5), C13−C14−C15 114.2(5); C5−C6−C7−C8 168.3(5), C6−C7−C8−C9 173.6(4), C7−C8−C9−C10 53.9(6), C8−C9−C10−C11 65.2(6), C9−C10−C11−C12 −169.1(4), C10−C11−C12−C13 64.4(7), C11−C12−C13−C14 63.4(7), C12−C13−C14−C15 −175.0(4)

The conformational behavior of $[(CH_2)_9(C_5H_4)_2]ZrCl_2$ in solution was characterized by dynamic NMR spectroscopy. In a $[D_8]$toluene solution, complex **3b** reveals spectroscopic data of apparent C_{2v} symmetry at ambient temperature, which is caused by a rapid conformational equilibrium on the NMR-spectroscopic time scale. At ambient temperature this leads to five $-CH_2-$ ^{13}C NMR resonances assigned to the *ansa* bridge at δ = 28.6, 26.6, 25.6, 24.6 and 23.7. The intensity of the latter signal is half that of the other signals. Under these conditions there are three Cp resonances at δ = 137.9 (*ipso*-C), δ = 111.7 and 115.7. The ^1H NMR spectrum (600 MHz) at "high" temperature (298 K) is similar, exhibiting methylene signals at δ = 2.40 (α-CH_2), 1.24 (8 H), 1.18 (2 H), and 1.13 (4 H) in addition to Cp methine signals at δ = 5.65 and 5.93. Lowering of the temperature eventually results in a freezing of the dynamic conformational equilibration process on the ^1H-NMR-spectroscopic time scale. Below 203 K (at 600 MHz), the well-separated ^1H NMR resonance of the methylene group in the α-position to the Cp ring system, begins to split into two signals of equal intensity that eventually appear at δ = 2.74 and 2.07 at 183 K. Under these static conditions the hydrogen atoms at the α-CH_2 group have thus become diastereotopic. Their nonequivalence indicates the presence of a single metallocene conformational minimum that is non-C_{2v}-symmetric. The remaining apparent C_s symmetry of the spectroscopically observed system may be real, or may be caused by a remaining very rapid local conformational symmetrization effect being operative in the medium-sized annelated nonamethylene ring system. In principle, a bis(lateral) conformation of **3b** in solution, similar to that observed in the crystal seems likely. Consequently, the pair of Cp ^1H NMR resonances broadens with decreasing temperature (Figure 4). Decoalescence is observed at ca. 203 K which results in the formation of two pairs of α,α′- and β,β′-C_5H_4 ^1H NMR resonances of equal intensity, at δ = 6.47/6.09 (3-H, 4-H) and δ = 5.09/4.92 (2-H/5-H). From these values a Gibbs activation energy of $\Delta G^{\ddagger}_{rot}(203\ K) = 8.8 \pm 0.3$ kcal/mol was obtained[20] for the conformational equilibration process of the "large" *ansa*-metallocene complex **3b** in $[D_8]$toluene. The conformational barrier is apparently not solvent-dependent. In the more polar solvent $CDFCl_2/CDF_2Cl$ (1:1),[21] a similar dynamic behavior was observed and an activation barrier of $\Delta G^{\ddagger}_{rot}(184\ K) = 8.5 \pm 0.3$ kcal/mol was obtained for the conformational equilibration process.

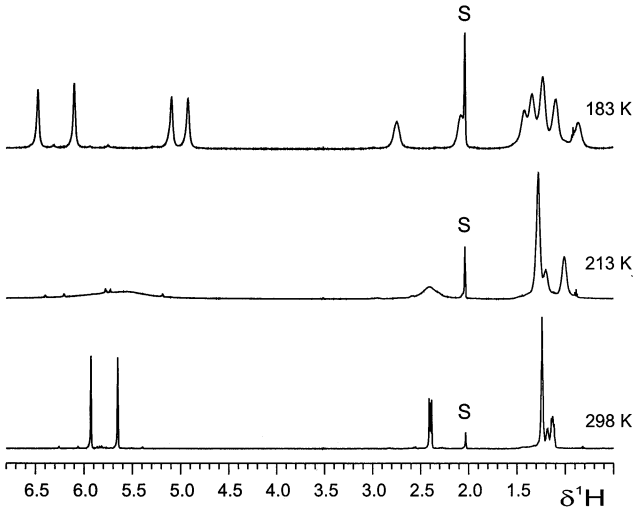

Figure 4. Dynamic ^1H NMR spectra (600 MHz) of **3b** in $[D_8]$toluene

From the dynamic NMR spectra it cannot be determined whether the C_9-oligomethylene chain moves through the front or back sector of the bent metallocene wedge during this conformational automerization process. From the computational energies of the $[(CH_2)_9(C_5H_4)_2]ZrCl_2$ system **3b**

that are compiled in Table 2, it appears that the nonamethylene chain may be accommodated slightly better at the back of the metallocene during such a migration process, although the respective ground-state energy differences are not prohibitively large and the transition-state energies were not calculated.

It can be assumed that steric interactions decrease for the dodecamethylene-bridged system $[(CH_2)_{12}(C_5H_4)_2]ZrCl_2$ (**3d**). Indeed, a similar 600-MHz ^{1}H NMR spectrum of **3d** was obtained at ambient temperature. In this case the conformational equilibration process of the "large" *ansa*-metallocene framework could not be frozen on the 600-MHz ^{1}H-NMR-spectroscopic time scale, even when the lowest temperature, 133 K, was reached (for spectroscopic details see the Exp. Sect.). It appears that the "large" *ansa*-metallocene complex **3d** exhibits dynamic properties similar to those of simple open, non-bridged alkyl-substituted group-4 bent metallocene complexes $[(prim.\text{-}alkyl)C_5H_4]_2ZrCl_2$ that are characterized by very low activation barriers for the conformational equilibration process.[22]

Olefin Polymerization Reactions

The combined conformational studies have shown that the complexes $[(CH_2)_9(C_5H_4)_2]ZrCl_2$ (**3b**) and $[(CH_2)_{12}(C_5H_4)_2]ZrCl_2$ (**3d**) attain favored conformations that have their long bridging oligomethylene chains oriented toward a lateral sector of the bent metallocene wedge, or that they are conformationally labile and may very easily turn away from the front sector. In any case, an active Ziegler−Natta catalytic system could be derived from such a singly bridged "large" *ansa*-metallocene that will allow for the unrestricted approach of reagents at the front sector of the bent metallocene wedge. This is essential for the catalyst's action, and we thus would expect that the systems **3b** and **3d** might lead to very active olefin polymerization catalysts on activation. This is indeed observed.

Activation of $[(CH_2)_9(C_5H_4)_2]ZrCl_2$ (**3b**) with methylalumoxane (MAO)[23] in toluene (Al/Zr ratio ca. 1800) at room temperature gave a very active homogeneous Ziegler−Natta catalyst for ethene polymerization. Polyethylene (m.p. 127 °C) was formed with an activity of $a \approx 2500$ kg polymer/mol [Zr]·h·bar (at 40 °C and 2 bar ethene pressure). The catalyst derived from complex $[(CH_2)_{12}(C_5H_4)_2]ZrCl_2$ (**3d**) was equally active in ethene polymerization under similar conditions ($a \approx 2400$). Both catalysts are also active in propene polymerization. Activation of **3b** was again achieved by treatment with a large excess of MAO (Al/Zr ≈ 1450). Polymerization at 40 °C (2 bar propene pressure) yielded ca. 21 g of an oily polypropylene with an activity of $a \approx$ 450 kg polypropylene/mol [Zr]·h·bar. The ^{1}H-NMR-spectroscopic analysis revealed that a low molecular weight oligomer was formed under these conditions. End-group analysis by ^{1}H NMR spectroscopy showed that an average 14-mer was obtained. The catalyst derived from the C_{12}-bridged "large" *ansa*-metallocene produced a similar propene oligomer (oligomerization degree of ca. 10 according to the NMR $H_2C{=}C(CH_3)-$ end group analysis)[24] with a catalyst activity of $a = 330$. The ^{13}C NMR pentade analysis showed that both polymers were atactic. The polypropylene formed at the **3b**/MAO-derived catalyst shows an mmmm ^{13}C NMR methyl pentade intensity of 6.7%, the material obtained at the **3d**/MAO catalyst 5.5% mmmm.

We conclude that the singly bridged "large" *ansa*-metallocenes studied in this work exhibit favored specific metallocene conformations if the bridging oligomethylene chains are small enough. Most often these chains are then found oriented toward lateral positions. Complexes with chain lengths of C_{12} or longer seem to be similar to non-bridged complexes.[25] The metal center in such monobridged systems is rather open and can easily be approached by external reagents. This results in rather active but stereochemically unselective Ziegler−Natta catalysts on activation with, for example, methylalumoxane. Bridge-specific effects will probably require a covalent fixation of a given metallocene conformation by the introduction of a second bridge.[6] It will be interesting to see how fixing a large $-(CH_2)_n-$ bridge in front of the bent metallocene alters the zirconocene behavior in an activated system. Such investigations and syntheses are actively being pursued in our laboratory.

Experimental Section

Computational Study: The force-field calculations were carried out with the program MAXIMOBY[26] using parameters based on the AMBER force field.[27] The parameters for the description of zirconium and its ligands in the $[Zr]Cl_2$ complexes were used as previously described by us.[9] A new set of parameters was deduced for the Zr−(sp^3-C) bond (carbon atom type MC) using 12 representative metallocene structures from the Cambridge Structural Database (details are provided with the Supporting Information). The following force-field data for the "new" carbon atom type MC were used (force constant in kcal mol^{-1}, reference values in Å or °): ZR−MC (110/2.275), HC−MC (330/1.09), MC−ZR−MC (80/95.5), MP−ZR−MC (80/104.2), XC−MC−ZR (5/109.5), HC−MC−ZR (40/109.5), −ZR−MC− (0/180.0, threefold) [MP denotes the artificial Cp(centroid) atom used in the metallocene force-field calculation and XC is the sp^2-carbon atom that is common to both the five- and six-membered ring of the indenyl ligand]. The starting geometries for the optimization were prepared using the visualization tool MOBY.[28] New conformations were generated within the MAXIMOBY program by breaking the central (sp^3-C)−(sp^3-C) bond of the oligomethylene chain, followed by changing the torsional angles successively by a 120° increment. Every new conformation was then optimized under the constraint that the ends of the resulting carbon chains formed initially after changing the torsion angles were not more than 6 Å apart to speed up the calculations. In addition the orientation of the ligands was changed systematically to provide different starting points for the force-field optimization procedures. The obtained results are listed in Tables 1−3. For additional information see the Supporting Information. − The validity of the force-field calculation was checked by a correlation with respective ab initio energies and ab initio conformational minimum structures. This was achieved by single-point calculations of all local minima of the obtained force-field structures by the DFT method B3LYP,[10] using the LAN L2DZ basis set. It contains a double-ζ valence basis set (8s6p4d)/[3s3p2d] with Hay and Wadt "effective core potentials" that substitute the Zr

electrons up to the 3d level,[29] and the Huzinaga−Dunning "double-ζ valence" basis set for the remaining atoms.[30] Resulting single-point energies and structures are provided in the Supporting Information. Results from the DFT optimizations are contained in Tables 1−3, and additional information (energies) are included in the Supporting Information. For details about the ZR-MC force-field parameterization, the force field and the DFT calculations see Supporting Information.

Synthetic Work. − General Information: Reactions with organometallic compounds were carried out under argon using Schlenk-type glassware or in a glove-box. Solvents (including deuterated solvents used for spectroscopic measurements) were dried and distilled prior to use. For additional general information, including a list of spectrometers used, see ref.[6] $ZrCl_4(THF)_2$,[31] 1,9-nonanediylbis(methanesulfonate) (**6b**),[32] and 1,12-dodecanediylbis(methanesulfonate) (**6d**)[33] were synthesized according to literature preparations. 1,9-Bis(cyclopentadienyl)nonane (**7b**) and 1,12-bis(cyclopentadienyl)dodecane (**7d**) were both obtained by procedures analogous to the literature preparations[34] of these compounds.

Preparation of 1,9-Bis(cyclopentadienyl)nonane (7b): Cyclopentadiene (4.10 mL, 49.4 mmol) was dissolved in 100 mL of THF at −15 °C. *n*-Butyllithium (28.5 mL of a 1.6 M solution in *n*-hexane, 45.6 mmol) was added dropwise, while stirring, over 1 h. The mixture was stirred for 3 h at 0 °C. A solution of 1,9-nonanediylbis(methanesulfonate) (**6b**) (6.00 g, 19.0 mmol) in 100 mL of THF was added dropwise at 0 °C (ice bath). The mixture was allowed to slowly warm to room temperature with stirring over a period of 12 h. Diethyl ether (75 mL) and a saturated aqueous sodium chloride solution (75 mL) was added, the organic phase separated and washed with water. The aqueous phase was extracted with ether (3×). The combined organic solutions were dried with anhydrous magnesium sulfate, filtered and concentrated in vacuo. Purification of the product was achieved by precipitation from acetone at −25 °C and gave **7b** as a pale yellow oil, as a mixture of isomers that exhibit the side chains at the 2- and 3-positions of the cyclopentadienyl rings. Yield of **7b**: 2.84 g (59%). − ^{1}H NMR (200.1 MHz, [D$_6$]benzene, 300 K): δ = 6.45 (m, 2 H, =CH), 6.34 (m, 1 H, =CH), 6.18 (m, 2 H, =CH), 5.92 (m, 1 H, =CH), 2.78, 2.68 (m, each 2 H, CH_2 of C_5H_5 of the two isomers), 2.38−2.26 (m, 4 H, 1-H, 9-H of the chain), 1.54−1.10 (m, 16 H, 2-H to 8-H of the chain). − ^{13}C NMR (50.3 MHz, [D$_6$]benzene, 300 K): δ = 149.7, 147.6 (C-1/C-2 of C_5H_5, two isomers), 135.1, 133.7, 132.8, 130.4, 126.8, 126.0 (=CH of C_5H_5, two isomers), 43.4, 41.4 (CH_2 of C_5H_5), 31.1, 30.3, 29.9 (double intensity), 29.3 (C1−C9).

1,12-Bis(cyclopentadienyl)dodecane (7d): The synthesis was carried out analogously as described above by treatment of cyclopentadiene (9.6 mL, 116.0 mmol) in 300 mL of THF with *n*-butyllithium (68.8 mL of a 1.6 M solution in *n*-hexane, 110.0 mmol) at −15 °C, followed by addition of a solution of 1,12-dodecanediylbis(methane sulfonate) (**6d**) (16.0 g, 53.6 mmol) in 200 mL of THF to give a ca. 1:1 mixture of two isomers of **7d** as an oil. Yield: 13.7 g (86%). − ^{1}H NMR (200.1 MHz, [D$_6$]benzene, 300 K): δ = 6.46 (m, 2H =CH), 6.33 (m, 1 H, =CH), 6.19 (m, 2 H, =CH), 5.97 (m, 1 H, =CH), 2.79, 2.70 (m, each 2 H, CH_2 of C_5H_5, two isomers), 2.39−2.27 (m, 4 H, 1-H, 12-H of the chain), 1.60−1.15 (m, 20 H, 2-H to 11-H of the chain). − ^{13}C NMR (50.3 MHz, [D$_6$]benzene, 300 K): δ = 149.2, 147.6 (C-1/C-2 of C_5H_5, two isomers), 135.1, 133.7, 132.6, 130.4, 126.8, 125.9 (=CH of C_5H_5, two isomers), 43.4, 41.1 (CH_2 of C_5H_5), 31.1, 30.3, 30.1, 30.0, 29.9, 29.4 (C-1−C-12).

1,9-Bis(lithiocyclopentadienyl)nonane (8b): *n*-Butyllithium (11.9 mL of a 1.6 M solution in *n*-hexane, 19.2 mmol) was added dropwise to a solution of 1,9-bis(cyclopentadienyl)nonane (**7b**) (2.08 g, 8.09 mmol) in 50 mL of diethyl ether at 0 °C. The mixture was stirred for 4 h at ambient temperature. The resulting white precipitate was collected by filtration, washed with ether (2 × 20 mL) and dried in vacuo to yield 2.02 g (93%) of **8b**, m.p. 176 °C (decomp.). − IR (KBr): $\tilde{\nu}$ = 3077 (w), 2926 (vs), 2853 (vs), 1463 (m), 1443 (m), 1077 (w), 1060 (m), 1041 (m), 1026 (m), 818 (s), 755 (vs) cm^{-1}. − $C_{19}H_{24}Li_2{\cdot}C_4H_{10}O$ (340.4): calcd. C 80.68, H 10.60; found C 80.98, H 9.90. − The product **8b** is insoluble in the usual solvents, even in the presence of 12-crown-4 crown ether. For further characterization it was therefore hydrolyzed with H_2O (a) or D_2O (b) and the resulting respective hydrocarbon products analyzed. − MS (70 eV): *m*/*z* (a) = 256 [M$^+$]; *m*/*z* (b) = 258 [M$^+$].

1,12-Bis(lithiocyclopentadienyl)dodecane (8d): The preparation was carried out analogously as described above by treatment of 1,12-bis(cyclopentadienyl)dodecane (**7d**), (9.18 g, 30.8 mmol) in 150 mL of diethyl ether with a solution of *n*-butyllithium (38.0 mL of a 1.6 M solution in *n*-hexane, 61.6 mmol), to yield 9.01 g (94%) of **8d**, m.p. 189 °C (decomp.) as an insoluble material. − IR (KBr): $\tilde{\nu}$ = 3079 (w), 2924 (vs), 2853 (vs), 1464 (m), 1367 (w), 1261 (w), 1089 (m), 1060 (m), 1041 (m), 1026 (m), 818 (s), 755(vs) cm^{-1}. − $C_{22}H_{30}Li_2{\cdot}2(C_4H_{10}O)$ (456.6): calcd. C 78.57, H 11.43; found C 78.75, H 11.13. − Hydrolysis with H_2O (a) or D_2O (b) was carried out analogously as described above to yield the respective hydrolysis products. − MS (70 eV): *m*/*z* (a) = 298 [M$^+$]; *m*/*z* (b) = 300 [M$^+$].

[1,9-Nonanediylbis(η^5-cyclopentadienyl)]zirconium Dichloride (3b): A suspension of $ZrCl_4(THF)_2$ (6.32 g, 16.8 mmol) in 100 mL of toluene was cooled to −78 °C and then slowly added to a cold (−78 °C) suspension of 1,9-bis(lithiocyclopentadienyl)nonane (**8b**) (4.50 g, 16.8 mmol) in 300 mL of THF. The mixture was allowed to warm to room temperature overnight, with stirring. The solvent was removed in vacuo. The orange colored residue was Soxhlet-extracted with pentane for 60 h to give **3b** as a grayish powder. Recrystallization from toluene at −30 °C gave **3b** as white crystals, yield 457 mg (7%), m.p. 198 °C. − $C_{19}H_{26}Cl_2Zr$ (416.5): calcd. C 54.79, H 6.29; found C 54.15, H 6.65. − IR (KBr): $\tilde{\nu}$ = 3100 (m), 2931 (vs), 2852 (s), 1487 (m), 1458 (m), 1439 (w), 1261 (m), 1096 (m), 1071 (m), 1053 (m), 1039 (m), 1029 (m), 875 (w), 853 (w), 818 (s), 732 (w) cm^{-1}. − The NMR assignments were supported by a series of 2D experiments (GHSQC, GHMBC, GCOSY);[35] the dynamic behavior of complex **3b** was examined by ^{1}H/^{13}C 1D and 2D NMR spectroscopy[20] in [D$_8$]toluene in a temperature range between 298 K and 183 K and by ^{1}H NMR in $CDFCl_2/CDF_2Cl$ (1:1)[21] between 253 K and 133 K. − ^{1}H NMR (599.9 MHz, [D$_8$]toluene, 298 K): δ = 5.93 (pseudo-t, 4 H, 3-H, 4-H of C_5H_4), 5.65 (pseudo-t, 4 H, 2-H, 5-H of C_5H_4), 2.40 (m, 4 H, 1-/9-H), 1.24 (m, 8 H, 2-/8-H and 4-/6-H), 1.18 (m, 2 H, 5-H), 1.13 (m, 4 H, 3-/7-H). − ^{13}C NMR (150.8 MHz, [D$_8$]toluene, 298 K): δ = 137.9 (C-1 of C_5H_4), 115.7 (C-3/C-4 of C_5H_4), 111.7 (C-2/C-5 of C_5H_4), 28.6 (C-1/C-9), 26.6 (C-2/C-8), 25.6 (C-3/C-7), 24.6 (C-4/C-6), 23.7 (C-5). − ^{1}H NMR (599.9 MHz, [D$_8$]toluene, 183 K): δ = 6.47 and δ = 5.09 (br., each 2 H, 3-H and 4-H of C_5H_4), 6.09 and 4.92 (br., each 2 H, 2-H and 5-H of C_5H_4), 2.74 and 2.07 (br., each 2 H, 1-H,H′ and 9-H,H′), 1.65−0.85 (m, 14 H, 2-H to 8-H). − Coalescence of 1-H,H′/9-H,H′ of the nonamethylene chain at ca. 203 K: Δν (183 K) = 399 Hz, $\Delta G^{\ddagger}_{rot}$ (203 K) = 9.0 ± 0.3 kcal mol^{-1}. Coalescence of the two groups of C_5H_4 proton resonances at ca. 203 K: Δν (183 K) = 701 Hz, $\Delta G^{\ddagger}_{rot}$ (203 K) = 8.8 ± 0.3 kcal mol^{-1}; Δν (183 K) = 828 Hz, $\Delta G^{\ddagger}_{rot}$ (203 K) = 8.7 ± 0.3 kcal mol^{-1}; averaged value in [D$_8$]toluene: $\Delta G^{\ddagger}_{rot}$ (203 K) = 8.8 ± 0.3 kcal mol^{-1}. − GHSQC NMR (599.9 MHz, [D$_8$]toluene, 183 K): δ (^{1}H)/(^{13}C) = 6.47/125.6, 6.09/115.6, 5.09/106.2, 4.92/106.5 (C_5H_4), 2.74/28.2,

Table 4. Ethene and propene polymerization reactions at the **3b**/MAO and **3d**/MAO catalysts

Precursor	Monomer[a]	mg (μmol) [Zr]	g (mmol) [Al]	Al/Zr ratio	Reaction time [min]	PE/PP[b] [g]	Activity[c]	m.p. (PE) n[d] (PP)
3b	E	8.0 (19.2)	2.1 (34.5)	1800	5	8.1	2540	127
3d	E	9.7 (21.2)	2.1 (34.5)	1630	5	8.6	2420	127
3b	P	9.8 (21.5)	2.1 (34.5)	1470	60	21.5	456	14
3d	P	10.1 (22.0)	2.1 (34.5)	1570	60	14.6	332	10

[a] All reactions were carried out at 2 bar monomer pressure at 40 °C. − [b] E = ethene, P = propene, PE = polyethylene, PP = polypropylene. − [c] Polymerization activity in kg (polymer)/mol [Zr]·h·bar. − [d] Oligomerization degree, determined by ^{1}H NMR end group analysis.

2.07/28.2, 1.45/23.5, 1.36/25.7, 1.36/22.3, 1.25/25.8, 1.24/23.5, 1.13/25.4, 1.10/22.3, 0.88/25.3 (CH_2). − ^{1}H NMR (599.9 MHz, $CDFCl_2/CDF_2Cl$, 253 K): δ = 6.45 (pseudo-t, 4 H, 3-H, 4-H of C_5H_4), 6.26 (pseudo-t, 4 H, 2-H, 5-H of C_5H_4), 2.67 (m, 4 H, 1-H, 9-H), 1.55−1.25 (m, 14 H, 2-8-H). − ^{1}H NMR (599.9 MHz, $CDFCl_2/CDF_2Cl$), 133 K): δ = 6.63 (br., 2 H), 6.36 (br., 4 H) and 6.30 (br., 2 H, C_5H_4), 2.68 and 2.46 (br., each 2 H, 1-H,H′, 9-H,H′), 1.38 (m, 14 H, 2-8-H). − 1-H,H′/9-H,H′ coalescence at ca. 183 K: Δν (133 K) = 132 Hz, $\Delta G^{\ddagger}_{rot}$ (183 K) = 8.5 ± 0.3 kcal mol^{-1}; coalescence of one group of C_5H_4 resonances at ca. 188 K: Δν (133 K) = 200 Hz, $\Delta G^{\ddagger}_{rot}$ (188 K) = 8.6 ± 0.3 kcal mol^{-1}. Averaged value in $CDFCl_2/CDF_2Cl$: $\Delta G^{\ddagger}_{rot}$(188 K) = 8.5 ± 0.3 kcal mol^{-1}.

X-ray Crystal Structure Analysis of 3b: Single crystals of complex **3b** were obtained by slow evaporation of solvent from a solution in benzene. Empirical formula $C_{19}H_{26}Cl_2Zr\cdot 1/2\ C_6H_6$, M = 455.57, colorless crystal 0.30 × 0.20 × 0.10 mm, a = 39.555(2), b = 6.512(1), c = 16.689(1) Å, β = 102.57(1)°, V = 4195.8(7) Å^3, $\rho_{calcd.}$ = 1.442 g cm^{-3}, μ = 7.81 cm^{-1}, empirical absorption correction via SORTAV (0.799 ≤ T ≤ 0.926), Z = 8, monoclinic, space group $C2/c$ (No. 15), λ = 0.71073 Å, T = 198 K, ω and φ scans, 19815 reflections collected (±h, ±k, ±l), [(sinθ)/λ] = 0.65 Å^{-1}, 4795 independent (R_{int} = 0.054) and 3448 observed reflections [I ≥ 2 σ(I)], 226 refined parameters, R = 0.054, wR^2 = 0.117, max. residual electron density 1.54 (−1.58) e Å^{-3} close to Cl1, Cl1 disordered over two positions, no disorder model used in the final refinement, hydrogen positions calculated and refined as riding atoms. Data set was collected with a Nonius KappaCCD diffractometer, equipped with a rotating anode generator Nonius FR591. Programs used: data collection COLLECT (Nonius B. V., **1998**), data reduction Denzo-SMN (Z. Otwinowski, W. Minor, *Methods Enzymol.* **1997**, *276*, 307−326), absorption correction SORTAV (R. H. Blessing, *Acta Crystallogr.* **1995**, *A51*, 33−37; R. H. Blessing, *J. Appl. Crystallogr.* **1997**, *30*, 421−426), structure solution SHELXS-97 (G. M. Sheldrick, *Acta Crystallogr.* **1990**, *A46*, 467−473), structure refinement SHELXL-97 (G. M. Sheldrick, Universität Göttingen, **1997**), graphics SCHAKAL (E. Keller, Universität Freiburg, **1997**). − Crystallographic data (excluding structure factors) for the structures reported in this paper have been deposited with the Cambridge Crystallographic Data Centre as supplementary publication CCDC-156106. Copies of the data can be obtained free of charge on application to CCDC, 12 Union Road, CambridgeCB2 1EZ, UK [Fax: (internat.) + 44-1223/336-033, E-mail: deposit@ccdc.cam.ac.uk].

[1,12-Dodecanediylbis(η^5-cyclopentadienyl)]zirconocene Dichloride (3d): A cold (−78 °C) suspension of $ZrCl_4(THF)_2$ (9.64 g, 25.6 mmol) in 250 mL of toluene was added to a suspension of the reagent **8d** (8.00 g, 25.8 mmol) in 600 mL of THF at −78 °C. The mixture was allowed to warm to room temperature overnight and then kept for 4 h at 60 °C. The solvent was removed in vacuo and the residue extracted (Soxhlet) with pentane for 60 h to give 2.06 g (18%) of **3d**, m.p. 144 °C. − $C_{22}H_{32}Cl_2Zr$ (458.6): caldc. C 57.62, H 7.03; found C 57.48, H 7.22. − IR (KBr): $\tilde{\nu}$ = 3102 (m), 2927 (vs), 2855 (s), 1488 (m), 1458 (m), 1439 (w), 1261 (w), 1094 (w), 1074 (w), 1052 (w), 1034 (m), 852 (m), 847 (m), 817 (s) cm^{-1}. − NMR assignments in [D_8]toluene were supported by GHSQC and GHMBC 2D NMR experiments[35] at 298 K. − ^{1}H NMR (599.9 MHz, [D_8]toluene, 298 K): δ = 5.85 (pseudo-t, 4 H, 3-H, 4-H of C_5H_4), 5.71 (pseudo-t, 4 H, 2-H, 5-H of C_5H_4), 2.42 (m, 4 H, 1-H/12-H of the chain), 1.35−1.23 (m, 20 H, 2-H to 11-H of the chain). − ^{13}C NMR (150.8 MHz, [D_8]toluene, 298 K): δ = 137.0 (C-1 of C_5H_4), 114.2 (C-3/C-4 of C_5H_4), 113.1 (C-2/C-5 of C_5H_4), 29.5 (C-1/C-12), 28.1, 27.7, 27.6, 27.4, 26.9 (C-2 to C-11). − The dynamic features of **3d** were examined by ^{1}H NMR spectroscopy in $CDFCl_2/CDF_2Cl$ in a temperature range between 253 K and 133 K; the 1-H,H′/12-H,H′ resonance shows the start of decoalescence at the lowest temperature reached (133 K). Since the temperature could not be lowered further in this solvent, the separated signals were not observed. − ^{1}H NMR (599.9 MHz, $CDFCl_2/CDF_2Cl$, 253 K): δ = 6.39 (pseudo-t, 4 H, 3-H, 4-H of C_5H_4), 6.19 (pseudo-t, 4 H, 2-H, 5-H of C_5H_4), 2.62 (m, 4 H, 1-H, 12-H), 1.63−1.27 (m, 20 H, 2-H to 11-H of the chain).

Olefin Polymerization Reactions: These were carried out in a toluene solution using a Büchi glass autoclave. Activation of the zirconocene dichlorides was carried out by treatment with a 10.5 w-% MAO solution in toluene, and the polymers worked up as previously described by us.[36] The ^{1}H NMR end group analysis of the polypropylene samples were carried out in 1,2,4-trichlorobenzene ([D_8]benzene lock) at 353 K. The stereochemical characterization was performed by ^{13}C NMR methyl pentade analysis.[24] Details of the polymerization experiments are compiled in Table 4.

Acknowledgments

Financial support from the Fonds der Chemischen Industrie and the Deutsche Forschungsgemeinschaft is gratefully acknowledged. We thank Dr. Christian Mück-Lichtenfeld for his help with the computational studies.

[1] Review: H.-H. Brintzinger, D. Fischer, R. Mülhaupt, B. Rieger, R. M. Waymouth, *Angew. Chem.* **1995**, *107*, 1255−1283; *Angew. Chem. Int. Ed. Engl.* **1995**, *34*, 1143−1171; see also: F. Piemontesi, I. Camurati, L. Resconi, D. Balboni, A. Sironi, M. Moret, R. Zeigler, N. Piccolravazzi, *Organometallics* **1995**, *14*, 1256−1266; H. Lee, P. J. Desrosiers, I. Guzei, A. L. Rheingold, G. Parkin, *J. Am. Chem. Soc.* **1998**, *120*, 3255−3256; J. C. Green, *Chem. Soc. Rev.* **1998**, *27*, 263−271, and references cited therein; H. G. Alt, E. Samuel, *Chem. Soc. Rev.* **1998**, *27*, 323−329.

[2] J. A. Smith, J. von Seyerl, G. Huttner, H. H. Brintzinger, *J. Organomet. Chem.* **1979**, *173*, 175−185; F. R. W. P. Wild, L.

Zsolnai, G. Huttner, H.-H. Brintzinger, *J. Organomet. Chem.* **1982**, *232*, 233−247; F. R. W. P. Wild, M. Wasiucionek, G. Huttner, H. H. Brintzinger, *J. Organomet. Chem.* **1985**, *288*, 69−77; F. Wochner, L. Zsolnai, G. Huttner, H. H. Brintzinger, *J. Organomet. Chem.* **1985**, *288*, 69−77; S. Collins, B. A. Kuntz, N. J. Taylor, D. G. Ward, *J. Organomet. Chem.* **1988**, *342*, 21−29; J. A. Ewen, R. L. Jones, A. Razavi, J. D. Ferrara, *J. Am. Chem. Soc.* **1988**, *110*, 6255−6256; P. Burger, J. Diebold, S. Gutmann, H.-U. Hund, H.-H. Brintzinger, *Organometallics* **1992**, *11*, 1319−1327; A. Razavi, J. L. Atwood, *J. Organomet. Chem.* **1996**, *520*, 115−120; G. M. Diamond, R. F. Jordan, J. L. Petersen, *J. Am. Chem. Soc.* **1996**, *118*, 8024−8033; M. Könemann, G. Erker, R. Fröhlich, S. Kotila, *Organometallics* **1997**, *16*, 2900−2908; R. L. Halterman, A. Tretyakov, M. A. Khan, *J. Organomet. Chem.* **1998**, *568*, 41−51.

[3] H. Lang, D. Seyferth, *Organometallics* **1991**, *10*, 347−349; T. K. Hollis, A. L. Rheingold, N. P. Robinson, J. Whelan, B. Bosnich, *Organometallics* **1992**, *11*, 2812−2816; R. L. Halterman, D. Combs, J. G. Kihega, M. A. Khan, *J. Organomet. Chem.* **1996**, *520*, 163−170; R. L. Halterman, D. Combs, M. A. Khan, *Organometallics* **1998**, *17*, 3900−3907; M. Ringwald, R. Stürmer, H. H. Brintzinger, *J. Am. Chem. Soc.* **1999**, *121*, 1524−1527.

[4] M. Knickmeier, G. Erker, T. Fox, *J. Am. Chem. Soc.* **1996**, *118*, 9623−9630; G. Erker, M. Aulbach, M. Knickmeier, D. Wingbermühle, C. Krüger, M. Nolte, S. Werner, *J. Am. Chem. Soc.* **1993**, *115*, 4590−4601.

[5] R. M. Waymouth, G. W. Coates, *Science* **1995**, *267*, 217−219; M. D. Bruce, G. W. Coates, E. Hauptmann, R. M. Waymouth, J. W. Ziller, *J. Am. Chem. Soc.* **1997**, *119*, 11174−11182; T. Dreier, G. Erker, R. Fröhlich, B. Wibbeling, *Organometallics* **2000**, *19*, 4095−4103.

[6] T. H. Warren, G. Erker, R. Fröhlich, B. Wibbeling, *Organometallics* **2000**, *19*, 127−134.

[7] M. Horáček, P. Štěpnička, R. Gyeped, I. Císařová, I. Tišlerová, J. Zemánek, J. Kubišta, K. Mach, *Chem. Eur. J.* **2000**, *6*, 2397−2408.

[8] G. Erker, C. Mollenkopf, M. Grehl, R. Fröhlich, C. Krüger, R. Noe, M. Riedel, *Organometallics* **1994**, *13*, 1950−1955.

[9] U. Höweler, R. Mohr, M. Knickmeier, G. Erker, *Organometallics* **1994**, *13*, 2380−2390.

[10] J. P. Perdew, *Electronic Structure of Solids '91* (Eds.: P. Ziesche, H. Eschrig), Akademie Verlag, Berlin, **1991**, p. 11; J. P. Perdew, J. A. Chevary, S. H. Vosko, K. A. Jackson, M. R. Pederson, D. J. Singh, C. Fiolhais, *Phys. Rev. B* **1992**, 46; J. P. Perdew, J. A. Chevary, S. H. Vosko, K. A. Jackson, M. R. Pederson, D. J. Singh, C. Fiolhais, *Phys. Rev. B* **1993**, 48; K. Burke, J. P. Perdew, Y. Wang, *Electronic Density Functional Theory: Recent Progress and New Directions* (Eds.: J. F. Dobson, G. Vignale, M. P. Das), Plenum, New York, **1998**; J. P. Perdew, K. Burke, Y. Wang, *Phy. Rev. B* **1996**, *54*, 16533; P. J. Stevens, J. F. Devlin, C. F. Chabalowski, M. J. Frisch, *J. Chem. Phys.* **1998**, 11623.

[11] For other applications of force-field calculations in metallocene chemistry see e.g.: A. K. Rappé, C. J. Casewit, K. S. Colwell, W. A. Goddard III, W. M. Skift, *J. Am. Chem. Soc.* **1992**, *114*, 10024−10035; J. R. Hart, A. K. Rappé, *J. Am. Chem. Soc.* **1993**, *115*, 6159−6164; H. Kawamura-Kuribayashi, N. Koga, K. Morokuma, *J. Am. Chem. Soc.* **1992**, *114*, 8687−8694; T. V. Timofeeva, J.-H. Lii, N. L. Allinger, *J. Am. Chem. Soc.* **1995**, *117*, 7452−7459; M. Toto, L. Cavallo, P. Corradini, G. Moscardi, L. Resconi, G. Guerra, *Macromolecules* **1998**, *31*, 3431−3438; D. Guo, X. Yang, L. Yang, Y. Li, T. Lin, H. Hong, Y. Hu, *J. Polymer Sci Part A: Polymer Chem.* **2000**, *38*, 2232−2238; N. Schneider, F. Schaper, K. Schmidt, R. Kirsten, A. Geyer, H. H. Brintzinger, *Organometallics* **2000**, *19*, 3597−3604; B. Bosnich, *Chem. Soc. Reviews* **1994**, *23*, 387−395; Reviews: T. R. Cundari, *J. Chem. Soc., Dalton Trans.* **1998**, 2771−2776; A. K. Rappé, W. M. Skift, C. J. Casewit, *Chem. Rev.* **2000**, *100*, 1435−1456; K. Angermund, G. Fink, V. R. Jensen, R. Kleinschmidt, *Chem. Rev.* **2000**, *100*, 1457−1470.

[12] G. Erker, K. Engel, U. Dorf, J. L. Atwood, W. E. Hunter, *Angew. Chem.* **1982**, *94*, 915−916; *Angew. Chem. Int. Ed. Engl.* **1982**, *21*, 914; U. Dorf, K. Engel, G. Erker, *Angew. Chem.* **1982**, *94*, 916−919; *Angew. Chem. Int. Ed. Engl.* **1982**, *21*, 914−915; V. Skibbe, G. Erker, *J. Organomet. Chem.* **1983**, *241*, 15−26; A. Stockis, R. Hoffmann, *J. Am. Chem. Soc.* **1980**, *102*, 2952−2962.

[13] L. Rossa, F. Vögtle, *Top. Curr. Chem.* **1983**, *113*, 1−86, and references cited therein.

[14] J. Y. Corey, X.-H. Zhu, L. Brammer, N. P. Rath, *Acta Crystallogr., Sect. C* **1995**, *51*, 565−567.

[15] C. Saldarriaga-Molina, A. Clearfield, I. Bernal, *J. Organomet. Chem.* **1974**, *80*, 79−90.

[16] A. Clearfield, D. Warner, C. Saldarriaga-Molina, R. Ropal, *Can. J. Chem.* **1975**, *53*, 1622−1629.

[17] C. S. Bajgur, W. R. Tikkanen, J. L. Petersen, *Inorg. Chem.* **1985**, *24*, 2539−2546.

[18] R. M. Shaltout, J. Y. Corey, N. P. Rath, *J. Organomet. Chem.* **1995**, *503*, 205−212.

[19] E. L. Eliel, S. H. Wilen, *Stereochemistry of Organic Compounds*, J. Wiley, New York, **1994**, p. 762−769, and references cited therein.

[20] M. L. H. Green, L.-L. Wong, A. Seela, *Organometallics* **1992**, *11*, 2660−2668, and references cited therein.

[21] J. S. Siegel, F. A. Anet, *J. Org. Chem.* **1988**, *53*, 2629−2630.

[22] G. Erker, T. Mühlenbernd, R. Benn, A. Rufińska, Y.-H. Tsay, C. Krüger, *Angew. Chem.* **1985**, *97*, 336−337; *Angew. Chem. Int. Ed. Engl.* **1985**, *24*, 321−323; R. Benn, H. Grondey, R. Nolte, G. Erker, *Organometallics* **1988**, *7*, 777−778; G. Erker, R. Nolte, G. Tainturier, A. Rheingold, *Organometallics* **1989**, *8*, 454−460; G. Erker, R. Nolte, C. Krüger, R. Schlund, R. Benn, H. Grondey, R. Mynott, *J. Organomet. Chem.* **1989**, *364*, 119−132; S. Knüppel, J.-L. Fauré, G. Erker, G. Kehr, M. Nissinen, R. Fröhlich, *Organometallics* **2000**, *19*, 1262−1268.

[23] H. Sinn, W. Kaminsky, *Adv. Organomet. Chem.* **1980**, *18*, 99−149. W. Kaminsky, K. Külper, H. H. Brintzinger, F. R. W. P. Wild, *Angew. Chem.* **1985**, *97*, 507−508; *Angew. Chem. Int. Ed. Engl.* **1985**, *24*, 507−508.

[24] Y. Inoue, Y. Itabashi, R. Chujo, Y. Doi, *Polymer* **1984**, *25*, 1640−1644; J. A. Ewen, *J. Am. Chem. Soc.* **1984**, *106*, 6355−6364, and references cited therein; M. Farina, *Top. Stereochem.* **1987**, *17*, 1−111.

[25] R. A. Howie, G. P. McQuillan, D. W. Thompson, *J. Organomet. Chem.* **1984**, *268*, 149−154; J. L. Petersen, L. F. Dahl, *J. Am. Chem. Soc.* **1975**, *97*, 6422−6433.

[26] MAXIMOBY Version 4.025, U. Höweler, Univ. Münster and CHEOPS, Altenberge, Germany.

[27] S. J. Weiner, P. A. Kollman, D. A. Case, U. C. Singh, C. Ghio, G. Alagoa, S. Profeta Jr., P. Weiner, *J. Am. Chem. Soc.* **1984**, *106*, 765; S. J. Weiner, P. A. Kollman, D. T. Nguyen, D. A. Case, *J. Comput. Chem.* **1986**, *7*, 230.

[28] MOBY Version 2.1A, U. Höweler, Univ. Münster and CHEOPS, Altenberge, Germany.

[29] P. J. Hay, W. R. Wadt, *J. Chem. Phys.* **1985**, *82*, 299−310; W. R. Wadt, P. J. Hay, *J. Chem. Phys.* **1985**, *82*, 284−298.

[30] T. M. Dunning Jr., *J. Chem. Phys.* **1971**, *55*, 716−723; T. M. Dunning Jr., *J. Chem. Phys.* **1970**, *53*, 2823−2833.

[31] L. E. Manzer, *Inorg. Synth.* **1982**, *21*, 136−140.

[32] C. F. H. Allen, J. P. Glauser, *Anal. Chem.* **1972**, *44*, 1694−1696.

[33] C. Mollenkopf, doctoral dissertation, Univ. Münster, Germany, **1993**; P. Cheng, A. Blumenstein, S. Subramanyam, *Mol. Cryst. Liq. Cryst. Sci. Technol. Sec. A.* **1995**, *269*, 1−38.

[34] J. K. Stille, L. Plummer, *J. Org. Chem.* **1961**, *26*, 4026−4029.

[35] S. Braun, H.-O. Kalinowski, S. Berger, *150 and More Basic NMR Experiments*, VCH, Weinheim, **1998**, and references cited therein.

[36] M. Dahlmann, G. Erker, K. Bergander, *J. Am. Chem. Soc.* **2000**, *122*, 7986−7998.

Received January 25, 2001
[I01033]